World Academy of Science, Engineering and Technology
International Journal of Biomedical and Biological Engineering
Vol:8, No:6, 2014

A Numerical Model for Simulation of Blood Flow in Vascular Networks

Houman Tamaddon, Mehrdad Behnia, Masud Behnia

***Abstract*—**An accurate study of blood flow is associated with an accurate vascular pattern and geometrical properties of the organ of interest. Due to the complexity of vascular networks and poor accessibility *in vivo*, it is challenging to reconstruct the entire vasculature of any organ experimentally. The objective of this study is to introduce an innovative approach for the reconstruction of a full vascular tree from available morphometric data. Our method consists of implementing morphometric data on those parts of the vascular tree that are smaller than the resolution of medical imaging methods. This technique reconstructs the entire arterial tree down to the capillaries. Vessels greater than 2 mm are obtained from direct volume and surface analysis using contrast enhanced computed tomography (CT). Vessels smaller than 2mm are reconstructed from available morphometric and distensibility data and rearranged by applying Murray's Laws. Implementation of morphometric data to reconstruct the branching pattern and applying Murray's Laws to every vessel bifurcation simultaneously, lead to an accurate vascular tree reconstruction. The reconstruction algorithm generates full arterial tree topography down to the first capillary bifurcation. Geometry of each order of the vascular tree is generated separately to minimize the construction and simulation time. The node-to-node connectivity along with the diameter and length of every vessel segment is established and order numbers, according to the diameter-defined Strahler system, are assigned. During the simulation, we used the averaged flow rate for each order to predict the pressure drop and once the pressure drop is predicted, the flow rate is corrected to match the computed pressure drop for each vessel. The final results for 3 cardiac cycles is presented and compared to the clinical data.

***Keywords*—**Blood flow, Morphometric data, Vascular tree, Strahler ordering system.

I. Introduction

ANY accurate hemodynamic analysis of blood flow must be established on detailed vascular circuit morphology of the organ of interest. The morphometric data on the branching pattern which determine connectivity of one branch to another and geometrical characteristics of the vascular tree including diameters, lengths and branching angles of the connected vessels must be determined to generate a proper model.

A basic difficulty, however, is that the pulmonary vascular tree consists of a large number of segments including a wide array of diameters and a complex branching pattern. Furthermore, due to the complex geometry of the vascular tree and technical limitations on general visualization techniques such as direct volume rendering and surface rendering using contrast enhanced computed tomography (CT) or magnetic resonance imaging (MRI), it is impossible to experimentally or clinically obtain a complete geometry of the entire vascular tree down to the capillary bed. Where the vessels of the pulmonary vascular tree become too small and more extensively networked that these methods fail to resolve structures or recognize the complex spatial relations of the vascular tree and its surrounding structures in detail. Hence, it is important to establish a platform for developing a full vascular tree from an incomplete image.

Morphometric data sets based on the Strahler ordering system [1]-[3] provide the most thorough characterization of the structure of arterial trees. Blood flow simulations for both steady and pulsatile flow have been performed in anatomic models created from morphometric data based on the Strahler ordering system [4], [5]. More recently, the diameter-defined Strahler ordering system was proposed [6] and has been used in studies of blood flow heterogeneity and input impedances [7]-[9]. Morphometry-based generated arterial trees are a proper candidate to provide the realistic anatomic and hemodynamic characteristics that will improve a patient-specific approach to modelling blood flow. While previously described methods for reconstructing morphometry-based arterial trees provide acceptable models for the missing parts of the vascular network, they make several assumptions that limit their accuracy to the realistic arterial tree. Most importantly, they assume that at each order of the vascular tree, segments have a constant diameter while the morphometric data report a spectrum for the size of the vessels at each order. Furthermore, the above mentioned methods do not consider the effect of branching angles in blood flow pattern. The benefits of obtaining an accurate computational model and simulation of the pulmonary vascular system are far from few. Experiments that would be impossible to run on live patients can be simulated limitless times through controlling input variables and parameters.

The presented approach facilitates the practical use of patient-specific computational models accurately as it utilizes current achievable clinical images for the main vessels and generates a realistic model for the distal vessels based on data that are not patient-specific, incorporating knowledge of vascular branching patterns and vascular characteristics in downstream networks based in anatomy. Lumped-parameter models, even though they are well suitable for representing compartments of the cardiovascular system when coupled to more detailed local models [10], do not directly describe the anatomy, leading to difficulties in choosing appropriate values for the parameters. Recent efforts have been made to develop

Houman Tamaddon and Masud Behnia are with the University of Sydney, Sydney, NSW 2006 Australia (e-mail: houman.tamaddon@sydney.edu.au, masud.behnia@sydney.edu.au).

Mehrdad Behnia is with Georgia Regents University, School of Medicine, Augusta, Georgia, USA (e-mail: doctorbehnia@gmail.com).

more accurate anatomic models of pulmonary vessels using a combination of medical images and morphometric data [11]. Meanwhile, fractal approaches have been used as an alternative for representing the distal anatomy [12]-[14], but the anatomic accuracy of their use of the same simple branching rules across the wide range of vascular network has been challenged[1].

In this study, we introduce a new three dimensional hybrid method in blood flow modelling of the pulmonary arterial tree incorporating a computational fluid dynamic (CFD) model of the proximal pulmonary arteries generated from three-dimensional medical imaging data. The model is coupled to the realistic hierarchical models of the distal orders based on morphometric data and tuned using the principle of minimum volume and Murray's laws. The intention of the present study is to develop a hybrid model to generate a full vascular pulmonary tree from an incomplete CT-based tree. Our approach is to use a CT-based geometry as a foundation and extrapolate the missing geometry on the distal parts using morphometric data. In the process, the proximal branches obtained from direct volume and surface rendering of the CT (including the main pulmonary artery down to 2 mm vessels) are completely known while the smaller vessels are artificially reconstructed order by order from the morphometric data and Murray's laws and distensibility of each segment is determined based on the modified diameter.

II. Methods

A. CT-Based Anatomic Model

A geometric model of the pulmonary arteries was created from a CT scan of the lung and refined using MeVisLab (MeVis Medical Solutions AG, Bremen, Germany), a cross-platform application framework for medical image processing and scientific visualization. It includes advanced algorithms for image registration, segmentation, and quantitative morphological and functional image analysis. The model consists of the pulmonary trunk, right and left pulmonary arteries, followed by a few generations of arterial branching before being truncated. This model was used as the proximal section of pulmonary tract, where the inlet of the total hybrid model is located at the pulmonary trunk. After generating the base model, statistical analysis was carried out on the model to determine an appropriate starting point for the downstream morphometric models. The distal arteries of the model were firstly categorised into orders based on cross sectional area. The implementation based on area was more appropriate than diameter due to the fact that some of the arteries were elliptical or disordered in cross section, rendering the parameter diameter inadequate. On the basis of this idea and to retain statistical consistency, the cross sectional area of the distal arteries were acquired and then classified according to the cross-sectional area ranges of each order determined from data published by [1]. Although some of the cross sections obtained from the arteries in the model did not fall within ranges from morphometric data, these were instead approximated to the closest order. Following the described process all distal vessels were assigned an order. **Error! Reference source not found.** shows the constructed geometry from CT scan.

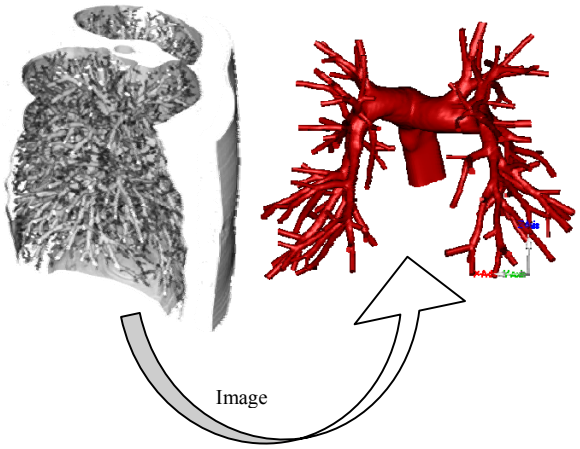

Fig. 1 Image processing result from a CT-Scan

B. Downstream Arterial Tree

The general template of the downstream models was devised on the basis of the connectivity data published by Huang et al. [1] which classified the entire pulmonary arterial network into 15 orders based on the diameter and the principle of minimum work by Murray [15]. We recall that the connectivity matrix is an array of values, where the number in the m^{th} row and n^{th} column is denoted by $\boldsymbol{C_{mn}}$, which represents the value for the average ratio of the number of elements of order m branching from elements of order n divided by the total number of elements in order n. Although the connectivity matrix defines the number of elements of order m branching from element n, it is not sufficient to describe a complete template due to the absence of information on the arrangement of the segments to the element, the distribution of the diameters in each order and the branching angles.

The problem of segment arrangement is overcome by defining our own set of rules to create a draft template from the element subtree matrix. To prevent confusion, we firstly define that the m^{th} row and n^{th} column denotes the number of order m segments branching from the element of order n. Continuing, we can thus describe that for a subtree of element order n, the element follows a continuous path where at a point it then bifurcates to two segments of order n-1. The remaining segment orders protrude from the element at alternating sides from junction points on the element and between the root of the element to the distal bifurcation point. Furthermore, the segments are arranged from largest order to smallest when they project from the element, with largest remaining segment projecting first and proximal from the element and vice versa. By describing the element structure in this way, the junction points in actual fact are also bifurcation points as they give off two segments. The element subtree thus has only one inlet for blood flow into the system and that all

branching segments are outlets.

As a result of these rules, we have identified that for a subtree of element order *n* the template is of an arrangement of segments coupled by bifurcation points, with the element section of the subtree being the segments that make up the core stem. The arrangement template also neglects the segments lengths, radii and bifurcation angles and thus is not to scale but rather illustrates a flexible general scaffold to be used in conjunction with tabulated parameter data for construction purposes. Moreover, because each different order element subtree ends with segments of an order below, we are essentially creating continuous sub trees of the pulmonary arterial tract.

C. Application of the Murray's Laws

Since we have identified an arrangement template for our downstream orders, the next step is the integration of the parameters such as branching angles and radii of each segment. Morphometric data is used to define the diameters of all the protruding segments and the first segment in the element; however for the later segments that make up the element section of the subtree we determine the radii by applying Murray's Laws with a cubic exponent[15].

$$r_0^3 = r_1^3 + r_2^3 \tag{1}$$

At the first bifurcation point the radii of the first element segment is known from morphometric data and acts as the parent, while the projecting segment and the following element segment act as the daughters. The projecting segment is again already defined by morphometric data, thus we can resolve the radii for the element segment. The following remainder of the element segment radii is determined by giving the daughter segment the role of the parent. The application of this law promotes the principle of minimum volume, as the element segments radii are reduced at each downstream bifurcation point. Checks with standard deviations for a specific order from morphometric data indicated that the radii determined using this method fall in those ranges, thus meaning that these element segments are indeed of the same order and valid.

After all segments in the subtree have had their radii defined, the branching angles at each bifurcation point can be determined using Murray's branching conditions for minimum work optimality [15].

$$\cos\theta_1 = \frac{r_0^4 - r_1^4 - r_2^4}{2r_0^2 r_1^2} \tag{2}$$

$$\cos\theta_2 = \frac{r_0^4 - r_2^4 - r_1^4}{2r_0^2 r_2^2} \tag{3}$$

The angles $\theta_1$and $\theta_2$in our case refers to the branching angles of the left and right daughters in a bifurcation, only the first segment that is the proximal segment before the first bifurcation point is of angle 0°. At each bifurcation prior to the final, the angle between the daughter branches to the axis of parent is calculated using the above equations. Similar to determining the radii using Murray's laws, the following latter bifurcation points are determined by giving each daughter element segment the role of the parent. The exception is that for the final bifurcation point the protruding segments of n-1 are given a branching angle of 37.475°. This is to coincide with Murray's investigations that for vessels of the same diameter the branching angles tend to be equal and are separated by 74.95° from one another.

D. Diameter–Pressure Relationship

The relationship between vessel diameter and pressure of human pulmonary arteries has not been extensively studied compared to other vascular structures in the human body. Many of the publications found in literature deal primary with establishing diameter vs. pressure changes of mammalian lung structures and extrapolating such results to the humans lungs. However, regardless of the species, it has been commonly agreed that the elasticity of the pulmonary arteries play a main role in dilation and contraction of such arteries.

Yen et al. [16] studied the elasticity of small pulmonary arteries in eight adult cats. After subjecting the lungs to a range of different perfusion pressures, they acquired data on pulmonary arteries on the range of 100-1600μm using x-ray film. They found that the pressure-diameter relationship was non-linear for arteries with diameters between 100-200 μm, whereas the larger arteries followed a linear relationship with a greater distensiblity. They also investigated the tendency for vessels to become elliptical when subjected to increasing pressure, and consequently data from extensive deformation of vessels were discarded. Using a similar technique, al-Tinawa et al. [17] demonstrated the distensibility of small pulmonary arteries of dogs, where they arrived at a parallel conclusion that there was a linear relationship between pressure and diameter in these vessels. Later, Hillier et al. [18] measured the pulmonary microvascular distensibility of vessels ranging in the size of 30-70μm using video microscopy. Videotaping the vessel diameter at the same location in each vessel under each experimental pressure, they found that the pressure-diameter relationship was mildly non-linear. They suggested that the non-linearity tends to be small over the physiological pressure range. They also observed larger vessels experiencing the same distensibility as the smaller vessels.

Following the success with the measurement of mammalian pulmonary arteries, Yen et al. [19] conducted measurements on the elasticity of arterioles and venules under 100μm in postmortem human lungs. Their studies were carried out on three sets of human lungs and prepared by selective perfusion with silicone elastomer. Firstly, they identified arterioles to be of order 1-3 under the Strahler hierarchy classification method. After highlighting the vessels, they set and maintained the airway pressure of the lungs to 10cm H_20 and established a gradient of transmural pressure $(P - P_A)$ of 0-17cm H_20 from the base to the apex of the lobe. Taking sections of tissues, the diameter variation of arterioles at various blood vessel pressures were measured. As such they established a linear relationship between pressure and diameter for the vessels of orders 1-3. The relationship can be

expressed as the following equation:

$$D = D_o + \alpha(P - P_A) \quad (4)$$

where D is the corresponding diameter, D_o is the initial diameter, α is the constant compliance, P the blood pressure and $P_A$the airway pressure. al-Tinawa et al. [17] report that there is consistency between distensibility results with 15 previous studies in cats, dogs, rabbits, rats and humans over the entire range of arterial diameters and thus stated that a value of α of $2\%D_o/\text{Torr}$ for the entire pulmonary arterial tree would appear to be a reasonable value based on the available data.

III. Binary Tree Generation

To establish a mathematical model of the pulmonary arterial network, we used diameter-defined Strahler system for assigning the order numbers of the vessels on the basis of diameter ranges. Each blood vessel between two successive points of bifurcation is called a *segment.* If several segments of a given order *j* are connected in series, then they are lumped together into a unit called an *element of order j*. Thus, the total number of elements of *order j* is smaller than the total number of segments of *order j*.

Custom software has been developed to generate a tree of pulmonary arteries for each end branch of the image-based model by applying the Murray's laws to the pulmonary morphometric data published by Huang et al. [1]. As described earlier, each end branch of the patient specific model is classified according to the cross sectional area ranges of each order, and a downstream tree is initialised using a chosen initial branch structure. The basic architecture of each segment and bifurcation is extracted from morphometric data and adjusted by applying Murray's laws. Once the dimensional and geometrical properties for each segment and its corresponding bifurcation are determined, the segment is labelled with a unique identification number which defines the hierarchical position of the segment, its parent and daughters.

The structure of the binary tree is designed to play three different roles. Firstly, it provides all the required data for geometry construction including connectivity, length, diameter and branching angle for each segment. Secondly, it is designed to record the hemodynamic properties of the flow through each segment during the simulation. In this stage, the binary tree plays as an interface between different solvers of different orders to share data during the simulation. Finally, the binary tree provides the post-processing toolbox implementing a path-tracing code for each downstream outlet.

The total number of the outlets of the reconstructed parts of the model was 15,949,316. The anatomical model terminated in 17 outlets of order 13, 68 outlets of order 12 and 38 outlets of order 11. A binary tree was generated for each end branch of the anatomical model and all structural and connectivity data were stored in a database. Forty nine minutes were required to generate the database for all 122 outlets of the anatomical model using COMPAQ VISUAL FORTRAN on a personal computer (3.2 GHz CORE i7, 32 GB RAM).

IV. Geometry Construction

Once all the geometric dimensions have been acquired, the construction process of the downstream models can begin. The CAD software, ANSYS Design Modeller was used to construct the sub trees, this is related to the fact there is support for parametric modelling with ease of integration into ANSYS CFX for simulation later without file format issues. The construction of the element sub trees of each order was built separately from one another, resulting in 12 different parametric sub trees starting from order 13. The initiative is a complete set of individual three dimensional models including the CT model that can represent flow from the pulmonary trunk inlet to the distal arteries before the capillaries. The construction process is separated into three key sections, the development of the Unit Scaffold, which then leads to forming the Merged Model and finally assembling the Integrated Model.

A. Unit Scaffold

To make the geometry construction process practical, we sought to divide the subtree into a smaller yet repetitive building block, defined as a "unit scaffold". The development of the unit scaffold follows our previous definition that the element subtrees are arrangements of segments separated by bifurcation points. Thus one can see that for each bifurcation junction, there is a parent segment followed by two daughter segments. If the bifurcation junction is not the final junction of the subtree, then one of the daughters would become a segment that is part of the element section of the subtree while the other becomes a protruding segment. Regardless, both daughters have the same physical relation to one another from the bifurcation standpoint. As such, we have defined one unit of an element subtree as a bifurcation junction with its respective parent and daughter segments. The idea is that the formation of the subtree is built by adding these units to the end of one another to form a subtree, where parameters are then manipulated to fit with tabulated dimensions corresponding to the order of the element subtree being modelled.

The unit scaffold was constructed in "ANSYS Design Modeller" using a wire frame approach. The key structures in the frame consist of the back bone which is the pathway from the start of the parent to the distal daughter segments and always lies equidistant from the vessel surface. It is used to characterize the lengths of the parent segment, bifurcation zone and the two daughter segments. The formulation of the scaffold is parametric meaning that all structures are dependent on another. The dimensions are also linked to a Microsoft Excel spread sheet and are given initial arbitrary values. The described scaffold is illustrated in Fig. 2.

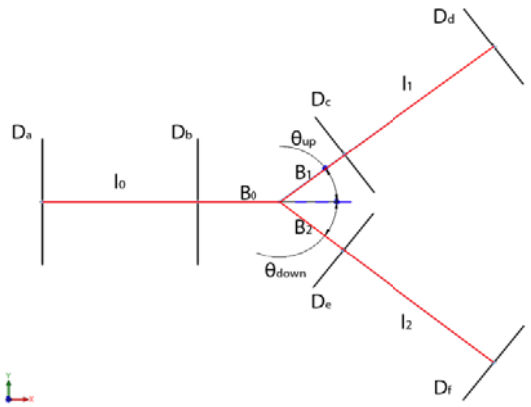

Where:	Definition
D_a, D_b	Start and end diameter of the parent segment
D_c, D_d	Start and end diameter of the up daughter segment
D_e, D_f	Start and end diameter of the down daughter segment
l_0	Length of the parent segment
l_1	Length of the up daughter segment
l_2	Length of the down daughter segment
θ_{up}	Branching angle for up daughter segment
θ_{down}	Branching angle for down daughter segment
B_0, B_1, B_2	Bifurcation zone lengths

Fig. 2 The Unit Scaffold

The bifurcation zone is a "Y" shape structure that is used to help define the branching angles and has an important role in distancing the parent segment from the daughter segments creating a junction. To convert the scaffold into a three dimensional structure the contours are lofted to one another. The result using this approach is a tree with segments represented by cylinders and merged via bifurcation junctions.

B. Merged Model

The merged model is essentially several unit scaffolds put together with imported element sub tree dimensions and lofted to form a three dimensional model of the sub tree itself. The procedure in accomplishing this follows firstly with building the element sub tree of order *n* using unit scaffolds to the form that it is in the arrangement template. Say, for example if we are building the element sub tree of order 6, it would constitute of two unit scaffolds with the down daughter segment of the first unit scaffold connected to the parent segment of the second unit scaffold. Thereby these two segments would form one segment and would share parameters. For further growth of the sub tree to other orders, unit scaffolds are added using the same process but to alternating ends of the previous unit scaffold each time.

Once the sub tree scaffold is complete, the parameters are linked to tabulated binary tree data and are automatically updated accordingly. The contours are lofted and a three dimensional model of the subtree is formed. A typical geometry of order 11 generated by this method is illustrated in Fig. 3. The procedure was applied to construct geometric models of all downstream orders with all parameters linked to the binary tree data acting as a data input medium. The method devised simplifies the construction process greatly due to the fact that each model is built using the same basic component, the unit scaffold, ridding the need for a different modelling procedure for each different order. Furthermore, the consistency in model detail from one another is kept.

Fig. 3 3D model of Subtree of Order 11

V. Integrated Model

The CT-based anatomic model and the morphometric-generated models provide a full representation of the pulmonary arterial tract. Thus to simulate blood flow within these models, the computational fluid dynamics solver (ANSYS CFX 14.5, Canonsburg) is used to simulate the blood flow of each model. The methodology undertaken consists of the blood flow in each order being simulated in individual solvers instead of being merged together as one whole model. This method not only facilitates the parametric simulation, but also simplifies the meshing procedure. This is because each model from order 2 to 13 and the CT model have individual length scales; hence, adequate meshing is better achieved and managed through separate simulations. These simulations are defined as "sub simulations" and integrated together they can simulate pulmonary arterial tract.

To better understand the methodology of simulation it is important to establish the direction of blood flow. Blood flow begins with perfusion into the pulmonary trunk in the CT model, which is then transferred to the smaller orders until the last order (which represent pre-capillary vessels) is reached. The concept is valid for each elemental sub tree model; blood flows from the proximal end and then exits the sub tree from all other protruding and distal segments. This means that for each model, there is only one inlet with several outlets. This is also true for the CT model where blood is perfused from the pulmonary trunk into the distal pulmonary arteries. For each time step, blood flow is simulated only once for each order and simulation results are interpolated for each vessel in the network based on its diameter. At this point, we developed an interface platform to integrate the CT model and all distal orders. This platform uses the binary tree structure as a shared database to transfer hemodynamic properties between different solvers during the simulation.

A. Geometry Callibration

As we used published morphometric data to reconstruct missing parts of the pulmonary vascular network and these data were based on limited number of experimental researches, we implemented a scaling algorithm to calibrate the reconstructed vascular tree by adjusting the sizes of vessels

for patient specific simulation. The aim of tuning the geometry is to achieve measured pre-operative pressure in the main pulmonary artery. The tuning was performed using a slightly modified method from one that was previously used by Spilker et al. [9] to tune impedance boundary condition. In brief, the diameters of the vascular elements of the tree were multiplied by β_D, in order to match the simulation's pressure to the measured value. The root pressure of the pulmonary artery is a function of blood flow and β_D.

$$P_{root,s} = f(Q_{in}, \beta_D) \quad (5)$$

Implementing the mean values over the cardiac cycle for simulated pressure ($P_{root,s}$) and blood flow (Q_{in}), we can define $g(\beta_D)$ as below:

$$g(\beta_D) = P_{root,s} - P_{root,m} = f(Q_{in}, \beta_D) - P_{root,m} \quad (6)$$

where $P_{root,m}$ is the mean value of the measured pressure. The solution of $g=0$ will indicate that simulation's pressure matches the measured clinical measurement. Note that each calculation of g requires a converged hemodynamic simulation.

Due to absence of an analytical solution for equation 6, we used a false position method for the solution of this nonlinear equation.

VI. Vascular Tree Statistics

As described earlier, once the node-to-node connections of the full tree was completely established and the diameters and lengths of every vessel segment assigned based on the diameter-defined Strahler system, the data on the diameters, lengths and branching angles were tabulated for every order number. The data on the daughter-to-mother connectivity were also determined. It should be noted that the matrices provide detailed connectivity data since they define which exact daughter element arises from which mother element. Finally, the analysed longitudinal positions of daughter vessels along the length of their mother vessel were computed. The present model represents the architecture of the entire pulmonary arterial tree. Every path length from the proximal pulmonary artery to the capillary was traced and the probability distribution of the various path lengths for three different crowns are shown in Fig. 4.

Crown of order 11:

Total number of

Segments: 62161
Bifurcations: 31080
End branches: 31081

Crown of order 12:

Total number of

Segments: 210353
Bifurcations: 105176 End branches: 105177

Crown of order 13:

Total number of

Segments: 713971
Bifurcations: 356985 End branches: 356986

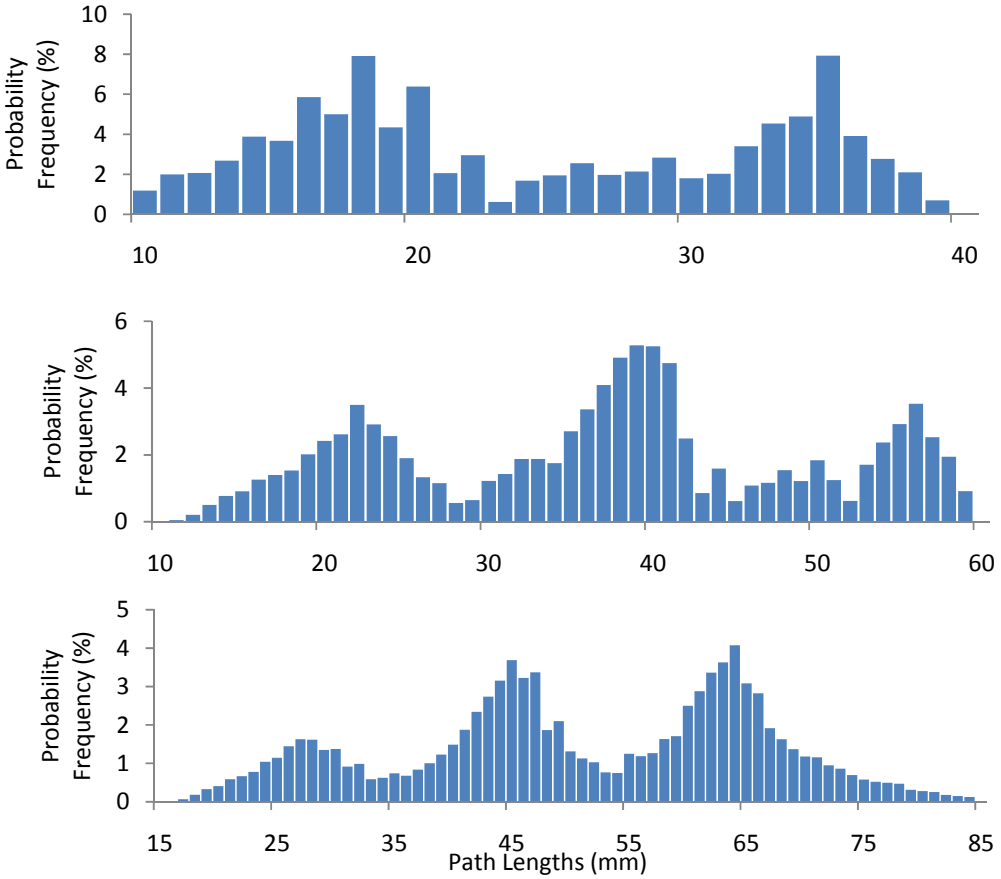

Fig. 4 Path Length Distribution for Different Crowns

Based on the minimum energy hypothesis and conservation of energy, Zhou et al. [20] previously showed that certain structure-structure relations exist. If A_s represents the mean cross-sectional area of a stem and V and L represent the

cumulative distal arterial volume and length of a crown, respectively, they derived the following equations:

$$V/V_{max} = \left(L/L_{max}\right)^{\gamma} \quad (7)$$

$$A_s/A_{s,max} = \left(L/L_{max}\right)^{\delta} \quad (8)$$

where $A_{s,max}$, V_{max} and L_{max} correspond to the cross-sectional area of the most proximal stem to the arterial tree, the volume of the entire tree of interest, and the cumulative arterial length of the entire tree, respectively; γ and δ are constants that can be determined from a curve fit of the statistical data. Similarly, the relationship between normalized stem cross-sectional area and normalized cumulative length of crown is shown for the same tree. Both relationships show a power law trend as described by (7) and (8), respectively. The average values of γ and δ for generated networks were 1.40 and 0.89, respectively.

VII. Simulation Results

Three-dimensional equations governing blood flow in an anatomic model of the pulmonary arteries with clinical inlet flow boundary conditions has been solved implementing a computational fluid dynamics solver (ANSYS CFX 14.5, Canonsburg). Simulations have been performed for three cardiac cycles with 200 time steps per cardiac cycle. Each vascular element was given the mean length value of its order in the morphometric data set and the diameter value was determined by applying the Murray's laws to the pulmonary morphometric data. The waveform flow with a mean value of 5.18 *L/min* was used as the inlet boundary condition for the simulation. The measured capillary wedge pressure, applied as the outlet boundary condition to the distal vessels, was 1892 *Pa*. Fig. 5 shows the simulation results for the maximum systolic flow rate in the main geometry and three different sub-trees.

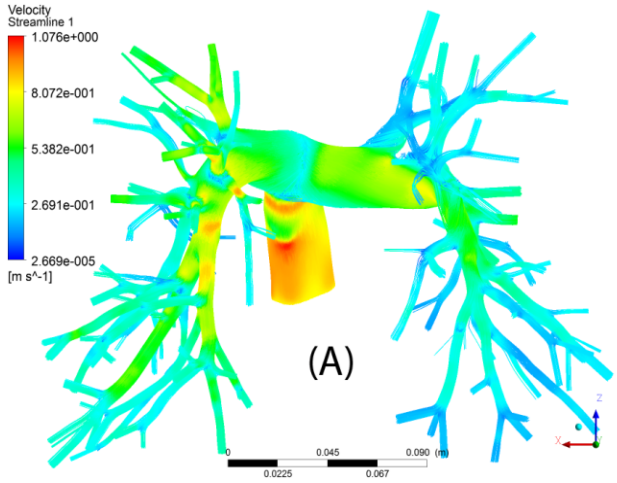

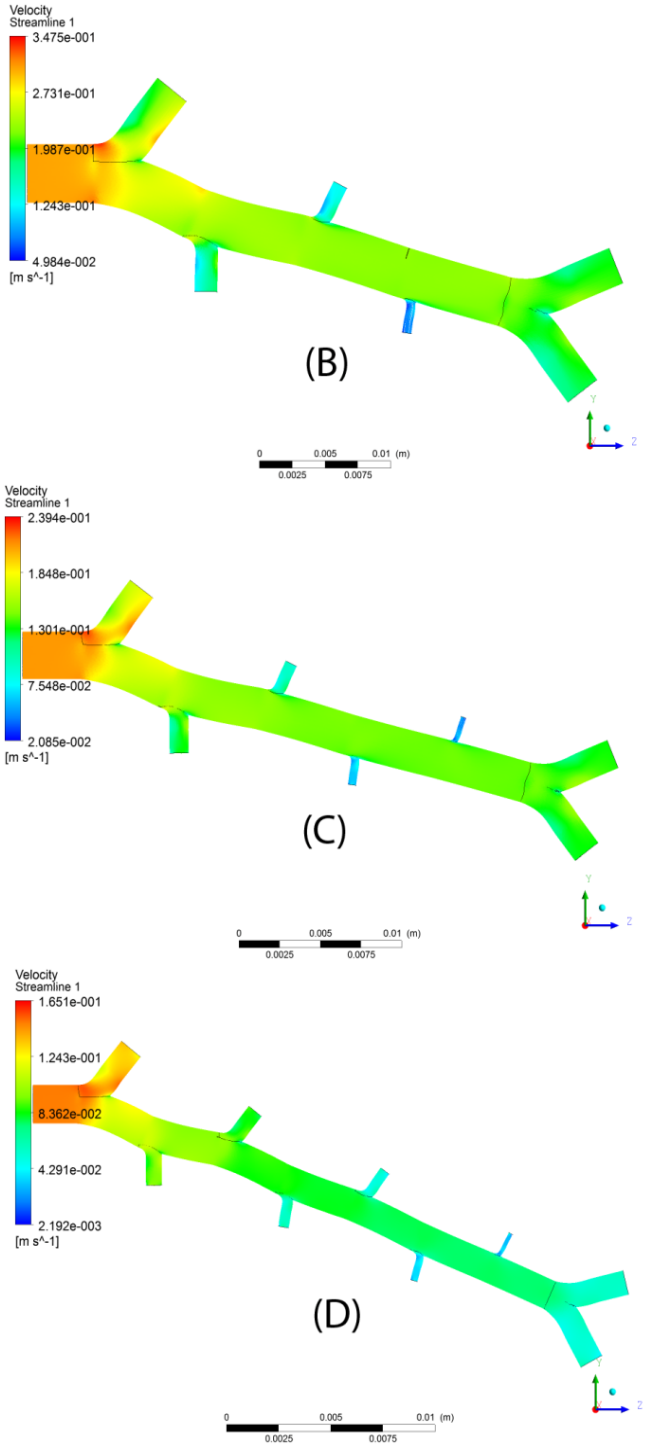

Fig. 5 Velocity Distribution through the Main Geometry (A), Vessel of Order 13 (B), Order 12 (C) and Order 11 (D)

The clinical measured value of mean pressure in the main pulmonary artery, was 2964 *Pa* (22.3 *mmHg*), and the initial simulation with morphometry-based distal network derived from this initial branch structure and β_D= 1, produced a mean pressure in the main pulmonary artery of 2719 *Pa*. The PA pressure waveform for the first simulation (before geometry calibration) is shown in Fig. 6.

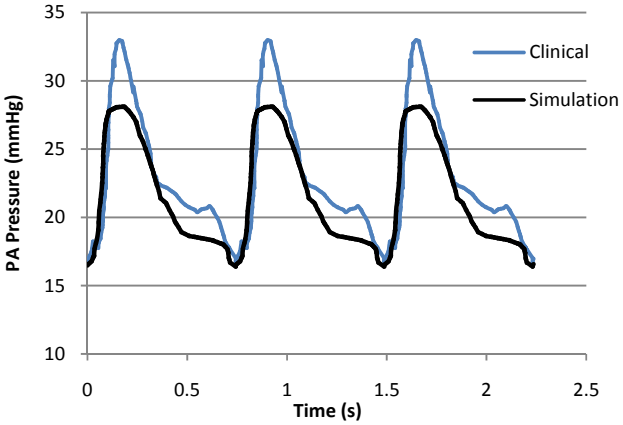

Fig. 6 PA Pressure Waveform before Geometry Calibration

After seven steps in the calibration process, the model's mean pressure was found to be within 2% of the clinical measurements on the eighth simulation. The pressure waveform measured in the main pulmonary artery and the corresponding simulation results for three cardiac cycles after tuning process are shown in Fig. 7.

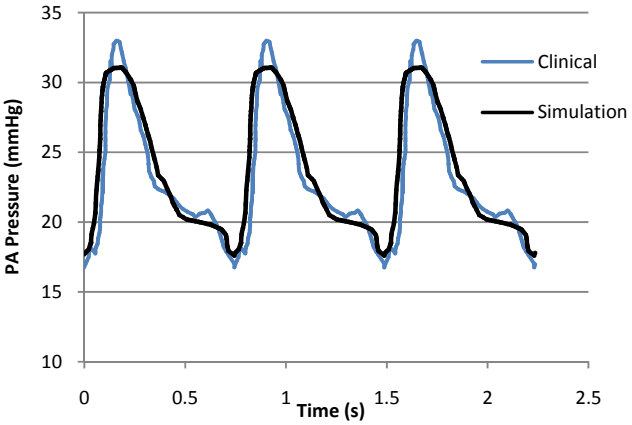

Fig. 7 PA Pressure Waveform after Geometry Calibration

After simulating the rest condition, inlet boundary condition was modified for exercise condition simulation. Generally, heart rate and stroke volume rise as a person starts to exercise and continue to rise as the intensity of the activity increases and as a result, cardiac output increases in a linear fashion to increases in the intensity of exercise, up to the point of exhaustion which is approximately three times of its value in normal condition. As no measurement were available for flow or pressure in exercise condition, rest condition flow wave form was multiplied by three to represent the exercise condition. In this simulation, the maximum pressure and average pressure rose from 4132 *Pa* and 2964 *Pa* to 5466 *Pa* and 3421 *Pa*, respectively. The rest condition pressure profile measured in the main pulmonary artery and the simulation results for exercise condition are presented in Fig. 8.

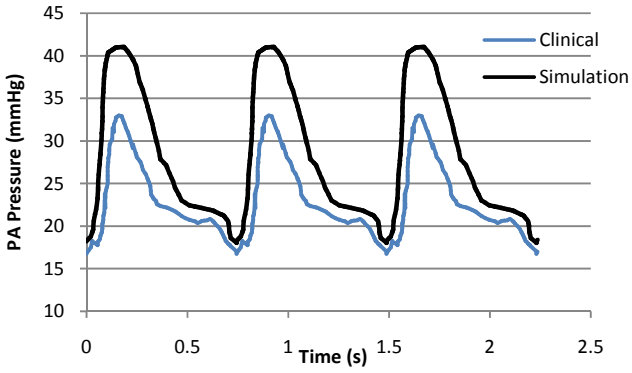

Fig. 8 PA Pressure Waveform for Exercise Condition

VIII. Discussion

In this study we developed a new method to represent the architecture of the entire arterial tree for the organ of interest, from the most proximal vessel segment to the inlet capillary vessels based on morphometric data. The anatomical geometry obtained from a CT image and the rest of the vessels were reconstructed as a group of sub-trees called crowns. Once the connectivity (node-to-node connections) of each crown was completely prescribed and the diameters and lengths of every segment determined, we used the diameter-defined Strahler system to categorise each crown to its building blocks named as Merged Model. The data on the diameters, lengths, branching angles and connectivity order (daughter-to-mother connectivity), were linked to the shared database. Finally, the statistical data for the entire tree were computed. Every path length from the proximal crown stem to the capillary can be traced. The morphometry-based arterial trees (sub-trees) were calibrated by dilating or constricting the vessels uniformly in each order such that the computed mean values of the main pulmonary artery pressure matched the clinical measurements.

Initially we used this method in an evaluating simulation (before calibration) which results showed the pressures in the simulation were lower than clinical measurements. After seven tuning steps and contraction of vessel diameters by about 7%, the simulation pressure was found to be within 2 % of the measured values. The results of the tuning process illustrate the sensitivity of the resistance of the arterial model to the diameters of the arteries. The calibrated model was later used to simulate exercise condition. Although no clinical data were available for the exercise condition, simulation results were reasonably accurate and compatible with the published data in the literature [21].

Validation of the use of the introduced model to accurately predict particular hemodynamic characteristics will require a series of *in vivo* experiments. It is notable that the arterial crowns developed from the diameters of the anatomic models' outlets led to reasonable pressures for the prescribed inlet flows in rest and exercise conditions, suggesting that the initial trees were valid starting points for the models. The differences in the clinically measured and numerically simulated pressure profiles may have resulted from a combination of model limitations, the use of linear elastic rather than viscoelastic

constitutive models for the vessel walls, inadequate morphometric data on pulmonary vasculature, and experimental limitations, such as the limited spatial and temporal resolution inherent in measuring the inlet blood flow or even the anatomical image resolution. Having access to more hemodynamic or anatomic information, proposed model could be modified to tune the method to better match simulated and experimental pressure and flow profiles in each segment of the lung. Implementing the proposed approach for patient-specific hemodynamic simulations can involve the selection of many parameters that cannot be evaluated *in vivo*. Using morphometry-based arterial trees, the matching process was simplified to the selection of a dilation factor for subtrees to satisfy the anatomic structure. In other words, this approach makes it possible to practically tune the boundary conditions for hemodynamic models of specific patients to approximate the available measurements.

A basic requirement of morphometry-based geometry reconstruction is analysis of typical morphometric and distensibility data. Arguably, the most important limitation of the morphometry-based pulmonary arterial model described in this method is the lack of such data for the pulmonary arteries of diseased patients such as patients with pulmonary arterial hypertension (PAH). Specifically, as previously noted [14], the current morphometric models of the distal vasculature, the vessels smaller than the current imaging resolution, are based on an idealized model derived from a single cast of a normal adult left lung. Each segment of the pulmonary arterial tree, whether it is the right upper lobe or left lower lobe, is then assigned the same geometry and features in the overall model. To date, there are no morphometric data available to define the unique characteristics of the various segments of the pulmonary arterial tree or to examine the effects of disease on the distal vasculature. Regardless of whether the vascular beds develop normally or abnormally, patient-specific solutions will ultimately require a more accurate model representing the various affected and unaffected segments within the lung. As knowledge of the effects of diseases on pulmonary arterial morphometry and distensibility becomes available, the methods we have described will be able to incorporate such data. In the meantime, the aforementioned tuning algorithm can be used to customize the generic morphometric data to the hemodynamic parameters of the patient.

REFERENCES

[1] Huang, W., R.T. Yen, M. McLaurine, and G. Bledsoe, *Morphometry of the human pulmonary vasculature.* Journal of Applied Physiology, 1996. 81(5): p. 2123-2133.

[2] Singhal, S., R. Henderson, K. Horsfield, K. Harding, and G. Cumming, *Morphometry of the Human Pulmonary Arterial Tree.* Circulation Research, 1973. 33(2): p. 190-197.

[3] Horsfield, K., *Morphometry of the small pulmonary arteries in man.* Circulation Research, 1978. 42(5): p. 593-7.

[4] Huang, W., Y. Tian, J. Gao, and R.T. Yen, *Comparison of Theory and Experiment in Pulsatile Flow in Cat Lung.* Annals of Biomedical Engineering, 1998. 26(5): p. 812-820.

[5] Zhuang, F.Y., Y.C. Fung, and R.T. Yen, *Analysis of blood flow in cat's lung with detailed anatomical and elasticity data.* Journal of Applied Physiology, 1983. 55(4): p. 1341-1348.

[6] Kassab, G.S., C.A. Rider, N.J. Tang, and Y.C. Fung, *Morphometry of pig coronary arterial trees.* American Journal of Physiology - Heart and Circulatory Physiology, 1993. 265(1): p. H350-H365.

[7] Gan, R.Z. and R.T. Yen, *Vascular impedance analysis in dog lung with detailed morphometric and elasticity data.* Journal of Applied Physiology, 1994. 77(2): p. 706-717.

[8] Kassab, G., J. Berkley, and Y.-C. Fung, *Analysis of pig's coronary arterial blood flow with detailed anatomical data.* Annals of Biomedical Engineering, 1997. 25(1): p. 204-217.

[9] Spilker, R., J. Feinstein, D. Parker, V.M. Reddy, and C. Taylor, *Morphometry-Based Impedance Boundary Conditions for Patient-Specific Modeling of Blood Flow in Pulmonary Arteries.* Annals of Biomedical Engineering, 2007. 35(4): p. 546-559.

[10] Laganà, K., R. Balossino, F. Migliavacca, G. Pennati, E.L. Bove, M.R. de Leval, and G. Dubini, *Multiscalemodeling of the cardiovascular system: application to the study of pulmonary and coronary perfusions in the univentricular circulation.* Journal of Biomechanics, 2005. 38(5): p. 1129-1141.

[11] Burrowes, K.S., P.J. Hunter, and M.H. Tawhai, *Anatomically based finite element models of the human pulmonary arterial and venous trees including supernumerary vessels.* Journal of Applied Physiology, 2005. 99(2): p. 731-738.

[12] Glenny, R.W. and H.T. Robertson, *A computer simulation of pulmonary perfusion in three dimensions.* Journal of Applied Physiology, 1995. 79(1): p. 357-369.

[13] Krenz, G.S., J.H. Linehan, and C.A. Dawson, *A fractal continuum model of the pulmonary arterial tree.* Journal of Applied Physiology, 1992. 72(6): p. 2225-2237.

[14] Steele, B.N., M.S. Olufsen, and C.A. Taylor, *Fractal network model for simulating abdominal and lower extremity blood flow during resting and exercise conditions.* Computer Methods in Biomechanics and Biomedical Engineering, 2007. 10(1): p. 39-51.

[15] Murray, C.D., *The physiological principle of minimum work applied to the angle of branching of arteries.* The Journal of General Physiology, 1926. 9(6): p. 835-841.

[16] Yen, R., Y. Fung, and N. Bingham, *Elasticity of small pulmonary arteries in the cat.* Journal of biomechanical engineering, 1980. 102(2): p. 170.

[17] al-Tinawi, A., J.A. Madden, C.A. Dawson, J.H. Linehan, D.R. Harder, and D.A. Rickaby, *Daistensibility of small arteries of the dog lung.* Journal of Applied Physiology, 1991. 71(5): p. 1714-1722.

[18] Hillier, S.C., P.S. Godbey, C.C. Hanger, J.A. Graham, R.G. Presson, O. Okada, J.H. Linehan, C.A. Dawson, and W.W. Wagner, *Direct measurement of pulmnarymicrovasculardistensibility.* Journal of Applied Physiology, 1993. 75(5): p. 2106-2111.

[19] Yen, R.T. and S.S. Sobin, *Elasticity of arterioles and venules in postmortem human lungs.* Journal of Applied Physiology, 1988. 64(2): p. 611-619.

[20] Zhou, Y., G.S. Kassab, and S. Molloi, *On the design of the coronary arterial tree: a generalization of Murray's law.* Physics in medicine and biology, 1999. 44(12): p. 2929.

[21] Kovacs, G., A. Berghold, S. Scheidl, and H. Olschewski, *Pulmonary arterial pressure during rest and exercise in healthy subjects: a systematic review.* European Respiratory Journal, 2009. **34**(4): p. 888-894.